Journal of Casting & Materials Engineering Vol. 6 No. 1 (2022) 22–32
https://doi.org/10.7494/jcme.2022.6.1.22

Strength, Water Absorption, Thermal and Antimicrobial Properties of a Biopolymer Composite Wound Dressing

Chiosa Cletus Odili[a*], Olatunde Israel Sekunowo[a], Margaret Okonawan Ilomuanya[b], Oluwashina Philips Gbenebor[a], Samson Oluropo Adeosun[a, c]

[a] University of Lagos, Faculty of Engineering, Department of Metallurgical and Materials Engineering, Nigeria
[b]University of Lagos, Faculty of Pharmacy, Department of Pharmaceutics and Pharmaceutical Technology, Nigeria
[c]Durban University of Technology, Durban South Africa, Industrial Engineering Department
**e-mail:* chiosa.odili@gmail.com

Received: 15 May 2021/Accepted: 8 February 2022/ Published online: 8 March 2022
This article is published with open access at AGH University of Science and Technology Press.

Abstract

Conventional wound material allows bacterial invasions, trauma and discomfort associated with the changing of the dressing material, and the accumulation of body fluid for wounds with high exudate. However, there is a shift from conventional wound dressing materials to polymeric nanofibers due to their high surface area to volume ratio, high porosity, good pore size distribution, which allows for cell adhesion and proliferation. There is an urgent need to synthesis a biodegradable composite that is resistant to bacterial infection. In this study, an electrospun polylactide (PLA) composite suitable for wound dressing, with enhanced antimicrobial and mechanical properties, was produced. The neat PLA, PLA/CH (10 wt.%), PLA/CH (5 wt.%), PLA/CHS (10 wt.%), PLA/CHS (5 wt.%), PLA/CH (2.5 wt.%) /CHS (2.5 wt.%) and PLA/CH (5 wt.%)/CHS (5 wt.%), were electrospun using 0.14 g/ml solution. Results show that crystallinity (67.6%) of neat PLA declined by 3.8% on the addition of 2.5 wt.% chitin/chitosan with improved hydrophilicity of the composite. The tensile strength of neat PLA (0.3 MPa) increased (0.6 MPa) with 2.5 wt.% chitin/chitosan addition. The slight increase in the glass transition temperature from 75°C for neat PLA to 78°C of the composite fibre, showed improved ductility. The fibres showed little beads, hence suitable for wound dressing. The electrospun mats have good water absorption capacity and strong resistance against *Staphylococcus aureus*. Good performance was attained at 5 wt.% of chitin, chitosan and hybrid reinforcements. Therefore, a PLA/chitin/chitosan composite is recommended as a wound dressing material.

Keywords:

chitin, chitosan, hydrophilicity, polylactide acid, skin, wound, staphylococcus-Auerus

1. INTRODUCTION

Wound healing is a global medical concern, and has thrown up other challenges, including the increasing incidence of obesity, type II diabetes, and ageing populations [1]. In 2018, retrospective analysis of Medicare beneficiaries identified that ~8.2 million people had wounds with or without infections. The Medicare cost estimate for acute and chronic wound treatment ranges from $28.1 billion to $96.8 billion. The highest expenses were for surgical wounds followed by diabetic foot ulcers [2]. In the US alone, over 100,000 surgeries performed daily involve surgical wounds. The anticipated market shares for wound care products are expected to reach ~US$25000 million. The use of growth factors to accelerate the healing of wounds offers a tremendous promise as a therapeutic approach in treating chronic wounds. Clinicians are unable to recommend the use of advanced dressings, however, because of their high cost, although these are more conducive to healing, require fewer dressing changes, and less care [3].

In terms of effectiveness, a wound dressing material should be able to keep the wound moist, stop bleeding, improve oxygen

absorption, remove exudates, be biodegradable, prevent bacterial infection and enhance the healing process [4–6]. The authors, [7] explicitly corroborated that wound dressings currently available in the Western Nigerian market do not fully address all the physiological issues associated with chronic wounds. The study primarily focused on bacterial clearance, leaving other factors inhibiting wound bed re-epithelization and wound closure unattended. It should be noted that a wound dressing material should be able to mimic the skin extracellular matrix (ECM). In this regard, nano fibres that are similar to ECM protein and pore size are important factors that facilitate cell respiration, haemostasis, exudate removal and moisture retention [8]. Electrospinning is considered one of the best methods of producing 3D nano-fibrous materials for the dressing of chronic wounds. Most electrospun fibres possess the desirable properties of an ideal wound treatment material. Although electrospinning is a simple and quick method in the fabrication of nano-fibrous scaffolds, there still exist challenges in the fabrication of scaffolds with complex structures, such as the homogeneous distribution of pores, thus limiting its application in biomedicine. In the study, [9] observed that the addition of particles can lead to the formation of a porous fibre network, which enables the material to absorb water and solvents. The introduction of new biopolymers and fabrication techniques that offer advantageous characteristics in wound dressing materials is important [8].

Polylactic acid (PLA) is obtained from natural raw materials such as maize and its degradation products including H_2O and CO_2. Their intermediate products, being hydroxyl and lactic acid, can be absorbed by the body [10, 11]. However, PLA has drawbacks like poor ductility and to improve on this property, it has been reinforced in recent times with different materials to form various composites. For example, [12] prepared a nano-fibre membrane of polylactic acid/polybutylene, carbonate/graphene oxide by electrospinning and noticed that the incorporation of graphene oxide (GO) leads to the improvement in the hydrophilicity of the PLA/PBC/GO membrane. This was attributed to the presence of the oxygen rich functional group in graphene oxide (GO), which reduces the highly hydrophobic ester group in PLA/PBC. Furthermore, [13] fabricated a novel high performance ductile polylactic acid nano scaffold coated with poly(vinyl alcohol) (PVA). The results showed that the nano-fibre demonstrated good hydrophilicity and mechanical properties. The study suggested that the improvement in the tensile strength was due to the increase in the tear resistance of the branch PVA fibres compared to the linear membrane rather than the presence of a physical/chemical bond between the polymers. Chitin (CH) and its derivative chitosan (CHS) are obtained from marine exoskeletons. Chitosan is known for its antibacterial, tumoricidal, natural blood clothing, wound healing and scar elimination properties [4]. Unfortunately, it is extremely difficult to electrospin chitosan, because of its high viscosity and polyelectrolyte nature [14] and specific intra and inter molecular interactions [15], which causes poor entanglement of the chains. Thus, chitosan is often blended with natural and synthetic polymers. From literature, there is little or no work on PLA/chitin/chitosan composite. PLA and chitin are known to be hydrophobic, while chitosan on the other hand is hydrophilic due to the amino group, therefore blending these biopolymers will enhance the hydrophilic behaviour of the composite. Thus, this work evaluates neat PLA, PLA/chitin, PLA/chitosan and PLA/chitin/chitosan fibre composites, to evaluate its physiochemical properties and ascertains their potential use in the management of surgical wounds around the abdominal region.

2. MATERIALS AND METHOD

2.1. Materials

Polylactic acid (average molecular weight 250,000 g/mol), dichloromethane 95% purity (England). Water used in all the tests was Milli-Q water (Millipore, USA). Bacterial strains of Methicillin-resistant *Staphylococcus aureus* obtained from South Africa was utilized in this study.

2.2. Method

14 g of PLA was dissolved in 100 ml of dichloromethane to produce solution of 0.14 g/ml viscosity. Then, 5 and 10 wt.% chitin and chitosan respectively were added to the solution and stirred continuously until homogenous mixture was achieved. This was followed by electrospinning at a constant voltage of 26 kV, with 90°C spinneret inclination at room temperature (28°C). A stationary Aluminum plate kept at 121 mm from the tip of the spinneret was used as the collector.

2.3. Characterization of electrospun fibre mat

2.3.1. X-ray diffraction (XRD)

The X-ray diffractometry measurements were performed using an EMPYERN diffractometer model XRD-600 at the National Geosciences Research Laboratory, Kaduna. The facility uses CuKα radiation (λ = 1.540598 Å, Ni-filter) at 40 kv, 30 mA. Without any preferred orientation, the samples were scanned in steps of 0.026261° in the 2θ in the range of 4.99–75.00° using a count time of 29.7 s per step.

The crystallinity index (*Crl*) for the neat PLA and the composites mats were calculated using Equation (1) [16].

$$Crl(\%) = \left(\frac{Ic}{Ic + Ia} \right) \times 100 \tag{1}$$

where *Ic* and *Ia* represent the intensities of the crystalline and the amorphous regions respectively.

2.3.2. Thermogravimetric analysis (TGA)

Analysis of samples was carried out on TGA Q500 instrument where 2 mg of samples were heated to 750°C at 10°C/min. The temperature for the onset of thermal decomposition (T_{onset}), temperature at the end of decomposition (T_{finish}) and the temperature at which decomposition was maximum (T_{max}) were deduced from the thermograms.

2.3.3. Scanning electron microscopy (SEM)

The micrographs of samples were produced via a scanning electron microscopy model Phenom Eindhoven, Netherlands situated at Amadu Bello University, Zaria. It works with an electron intensity beam of 15 kV, while the samples were mounted on a conductive carbon imprint left by the adhesive tape. This is usually prepared by placing the samples on the circular holder and coated for 5 min to enable it conduct electricity. Free online software, Image J was used to determine the pore size and fibre diameter of electrospun mats.

2.3.4. Differential scanning calorimetry (DSC)

Thermal characteristics of 7–8 mg of the electrospun samples were determined using a differential scanning calorimetry (DSC) device (Mettler Toledo Equipment DSC1 star system) operated from 25 to 250°C at 10°C/min. High pressure pans were used for the test and heat flow was measured as a function of the temperature and time.

2.3.5 Tensile test

Tensile strength characteristics of the neat PLA and the composites mats were determined using an Instron 3369M tensometer located at the Centre for Energy Research and Development, Obafemi Awolowo University, Ile-Ife Nigeria. Each sample was fixed and held firmly at both ends by the gauge as the load was applied until the sample finally failed.

2.3.6. Water absorption test

Water absorption of the fibre mat was studied at room temperature. Electrospun fibres were weighed and immersed in 50 ml of water for one month. During this period, the sample was removed from the water, cleaned and reweighed every one week. At the end of the one-month interval, the water absorption was calculated using Equation (2) [17].

$$Water\ uptake\ (\%) = 100 \times \frac{W_{wet} - W_o}{W_o} \tag{2}$$

where:

W_{wet} – is weight of wet fibre;
W_o – initial weight of the sample prior to immersion.

2.3.7. Antibacterial assay

An antibacterial susceptibility test was conducted using several pieces of equipment and tools including an autoclave model YX-280A, a Gallenkamp incubator model from England, a weighing balance manufactured by Ohaus, micropipette, nutrient agar and peptone water (Lab M, UK), petri dishes, cotton wool, antibiotic, *Staphylococcus aureus strain* (ATCC 29213), forceps and a Bunsen burner. The antibacterial assay of the composites was performed on *Staphylococcus aureus* strain (ATCC 29213), which was maintained in glycerol-nutrient broth at 4°C in the Department of Microbiology, University of Lagos, Nigeria. According to a modified protocol by [18], the bacterial strain was sub-cultured in peptone water (Lab M, UK) and incubated at 37°C for 24 h. The culture was serially diluted, and aliquot of appropriate dilution was inoculated into fresh sterile peptone water in McCartney bottles corresponding to the test samples. The composites were incorporated into the inoculated medium with the aid of a sterile pair of forceps. The samples were further incubated at 37°C for 24 h. To determine the total viable counts (TVCs), five folds' serial dilutions of the test samples and controls were made. Aliquot of appropriate dilutions of the test samples and controls were plated onto nutrient agar plates (Lab M, UK) in duplicates using the pour plate technique [19]. The inoculated plates were then incubated at 37°C for 24 h. After 24 h incubation, the developed colonies were counted in duplicates, and the mean values were multiplied by the dilution factor to give TVC. The bacterial colony forming units (CFUs) were compared with the bacteria growth in the absence of the composites (organism control).

3. RESULTS AND DISCUSSION

3.1. Effect of reinforcement on crystallinity of PLA composite fibres

Neat PLA (see Fig. 1) was used as a reference to the entire composite fibre mats. A weak and broad scattering reflection, with low absorption intensity attributed to several degrees of molecules deformation [20] was detected around 2θ = 16.7° and 19.5° for the neat PLA. This is within the range reported by [21] for semi crystalline polymer. Crystalline peaks for chitin and chitosan occurred around 2θ range of 16.5° and 22.5°. This was also observed by [15]. This may be attributed to the intercalation of chitin and chitosan structure within the PLA matrix. However, there was no change in the crystalline peak position for the composite mats at various percentages of reinforcement, when compared with neat PLA. This shows good miscibility and interactions between the composite constituents. This interaction might have occurred due to the hydrogen bonding between the PLA and hydroxyl/amine group of chitin (CH) and chitosan (CHS). A narrow hump was noticed at 2θ range of 33° for the fibre mats with PLA/CH (10 wt.%) and PLA/CH (2.5 wt.%) /CHS (2.5 wt.%). The crystallinity index of the fibre mats is shown in Table 1. The high degree of crystallinity of the electrospun neat PLA and PLA/CHS (5 wt.%) fibres when compared to the other composites was ascribed to the higher stretching of the polymer chains leading to a higher degree of molecular organization [22]. Adding a hybrid of chitin and chitosan at varying weight percentages lowers the degree of crystallinity of PLA by 3.8%. [23] observed that the crystallinity of PLA decreased by 2 and 8% when it was reinforced with 10 and 35 wt.% of Titanium oxide respectively. The lower degree of crystallinity improves degradability, and solves the hydrophobic problem of PLA, which is a key factor in improving drug release and drug loading efficiency [24, 23] thus, making the fibre mats useful for wound dressing.

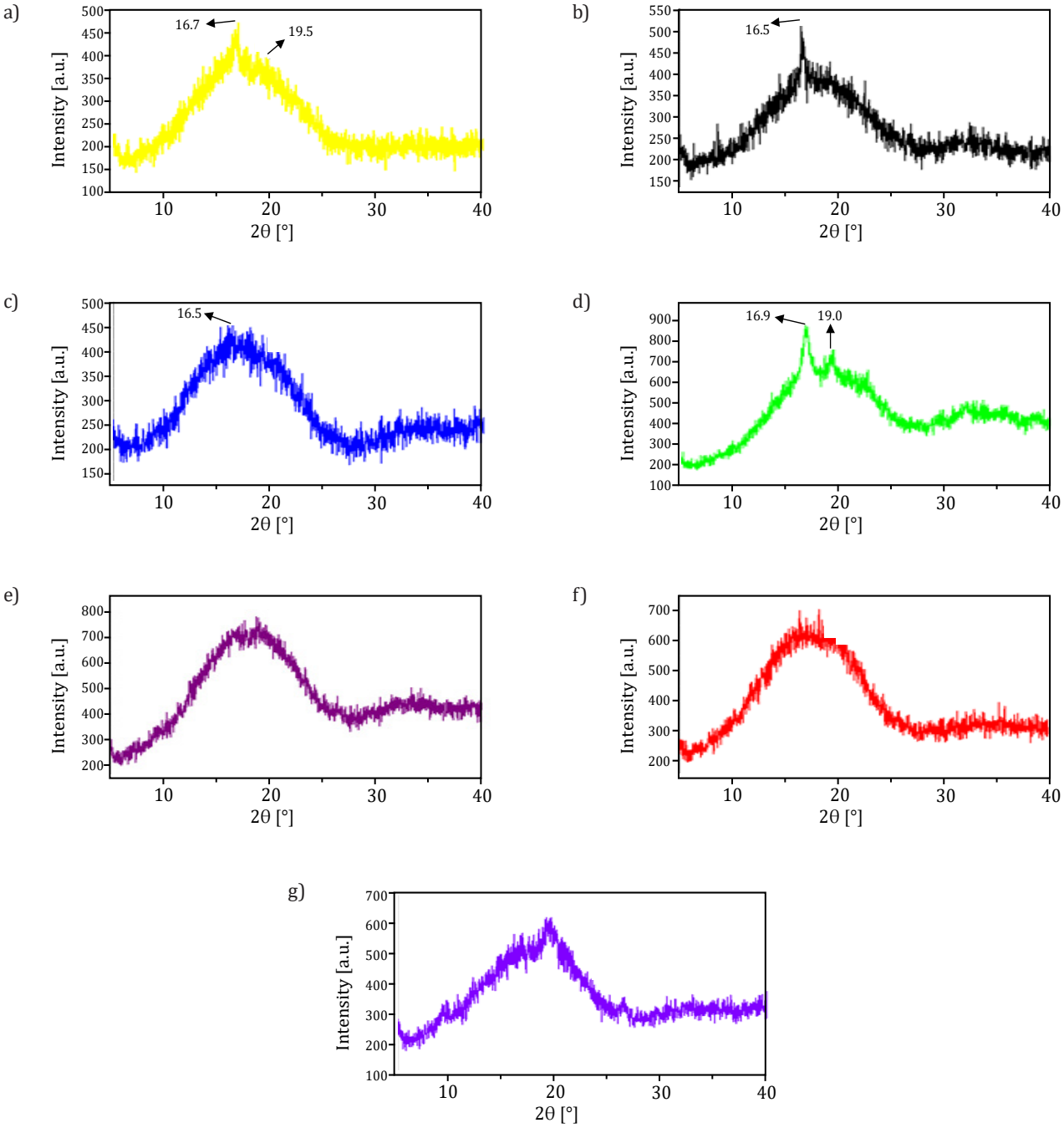

Fig. 1. XRD of electronspun PLA and composite fibre: a) neat PLA; b) PLA/CH (5 wt.%); c) PLA/CHS (5 wt.%); d) PLA/CH (2.5 wt.%)/CHS (2.5 wt.%); e) PLA/CH (10 wt.%); f) PLA/CHS (10 wt.%); g) PLA/CH (5 wt.%)/CHS (5 wt.%)

Table 1
Crystallinity of the electrospun fibre

Electrospun fibre	Crystallinity [%]
PLA	67.6
PLA/CH (10 wt.%)	65.1
PLA/CH (5 wt.%)	67.1
PLA/CHS (10 wt.%)	66.7
PLA/CHS (5 wt.%)	67.6
PLA/CH (2.5 wt.%) /CHS (2.5 wt.%)	65.3
PLA/CH (5 wt.%)/CHS (5 wt.%)	65.8

3.2. Thermal degradation response of the reinforced PLA composite

The TGA thermogram (see Fig. 2) of neat PLA showed a range of thermal degradations between 311–364^{0}C with initial mass loss of 25% and 43%. This degradation temperature for neat PLA falls within the range reported by earlier researchers [25, 26]. The residue decomposes finally at 542°C. The fibre mat composites showed, thermal degradation of 301–379°C, 272–348°C, 257–339°C, 287–416°C, 287–405°C and 292–377°C, for PLA/CHS (10 wt.%), PLA/CH (2.5 wt.%)/CHS (2.5 wt.%), PLA/CHS (5 wt.%), PLA/CH (5 wt.%), PLA/CH (5 wt.%)/CHS (5 wt.%), PLA/CH (10 wt.%) respectively. The degradation temperature of chitin has been found to occur around 400°C. [27–29] reported that chitosan exhibited two stages of degradation, with the loss of water molecules in the first stage. However, this result does not agree with what was observed in the present study, where three stages of decomposition were observed. The first stage, which is the loss of water molecules due to hydrophilic nature of chitin and chitosan, was not visible in these spectra, since their percentage in the matrix was relatively small and it also confirms that there was complete vaporization of Dichloromethane after electrospinning. The second stage is at 342–369°C, with the decomposition of the pyranose ring along the polymer backbone to form a complex adduct. The third stage was at 417–415°C, and is the decomposition of the obtained adducts. This is consistent with the works of [15, 30] where it was reported that the thermal stability of electrospun chitosan reinforced with chitin nanocrystals is 180°C. A similar thermal stability of ~185°C was obtained in this present study. The studies suggest that all the fibres have the required thermal stability to be used in wound dressing, which will be in-contact with the body.

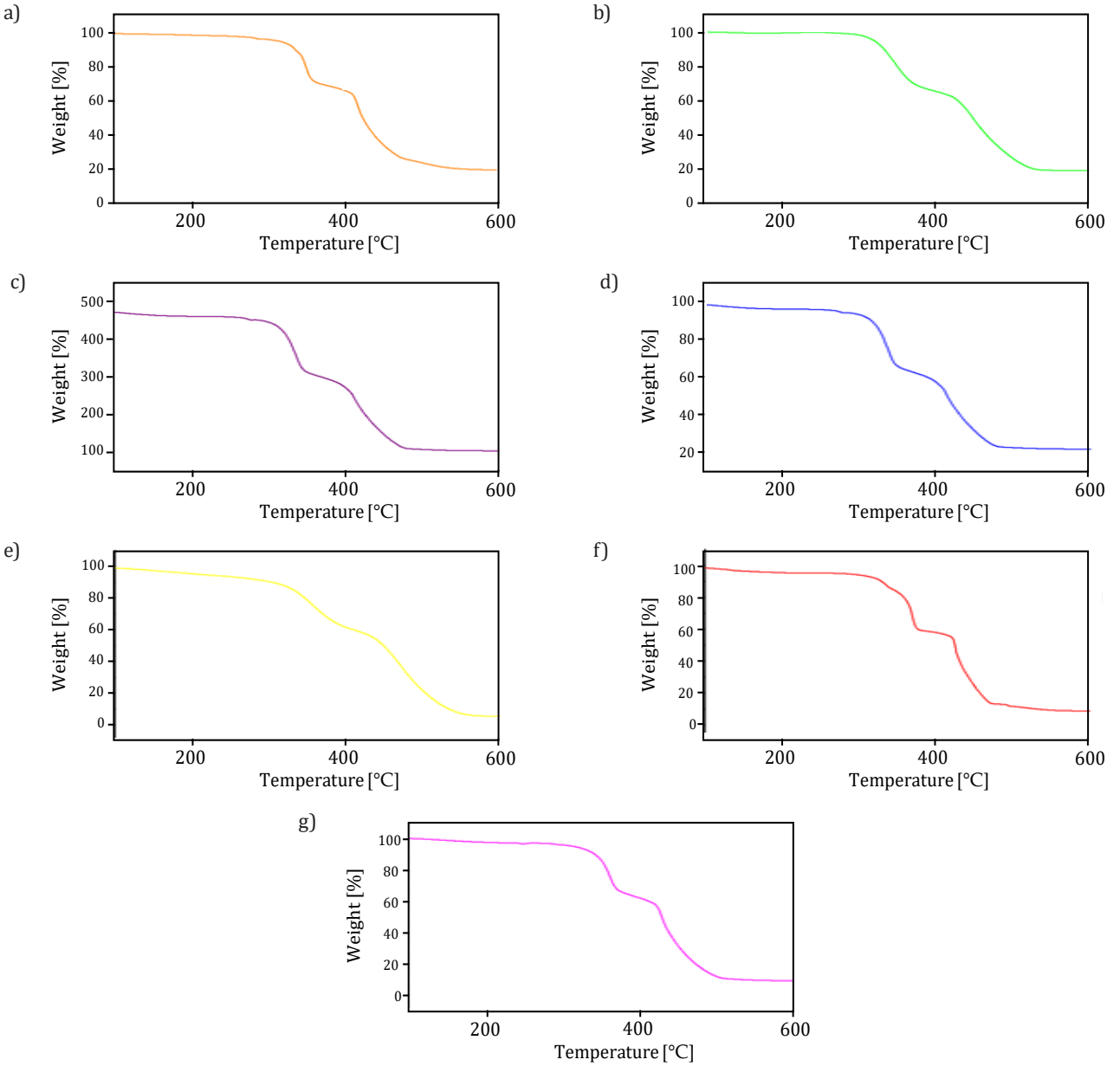

Fig. 2. TGA of electrospun PLA and the fibre mat: a) neat PLA; b) PLA/CH (5 wt.%); c) PLA/CHS (5 wt.%); d) PLA/CH (2.5 wt.%)/CHS (2.5 wt.%); e) PLA/CH (5 wt.%)/CHS (5 wt.%); f) PLA/CHS (10 wt.%); g) PLA/CH (10 wt.%)

From the TGA curve (see Fig. 2), it was observed that, the neat PLA fibre is more thermally stable than the fibre mats of PLA/CHS (10 wt.%), PLA/CH (2.5 wt.%) /CHS (2.5 wt.%), PLA/CHS (5 wt.%), PLA/CH (5 wt.%). This is consistent with the works of [31, 32]. According to the authors [15] who reinforced PLA with PVA, they observed that the decomposition temperature of the composite was reduced in comparison with the neat PLA. This result also showed that the compatibility and interfacial bonding decreases by mixing of both PLA polymer and fibre [32]. The presence of the fibre in PLA destabilized the PLA matrix, where some portion of the polymer is replaced with less thermally stable fibres in the composite materials [31]. In the study, [33] attributed this to the thermal instability of PLA. The reduction in thermal stability does not alter the properties of the scaffold when used at biological temperatures (37°C) [34] and is therefore deemed insignificant in practical terms [35]. Conversely, PLA/CH (5 wt.%) and PLA/CH (5 wt.%) /CHS (5 wt.%) were more stable when compared with the neat PLA; this may be attributed to pronounced particle interaction within the fibre matrix. Similar results were also obtained by [36, 37].

3.3. Decomposition characteristics of PLA fibre composites

The DTG thermogram (see Fig. 3) showed maximum decomposition temperature at 399°C, 483°C, 385°C. 411°C, 378°C, 403°C, 409°C for Neat PLA, PLA/CH (5 wt.%)/CHS (5 wt.%), PLA/CHS (5 wt.%), PLA/CH (10 wt.%), PLA/CH (2.5 wt.%)/CHS (2.5 wt.%), PLA/CH (5 wt.%) and PLA/CHS (10 wt.%), respectively. Thus, some of the composites (478°C, 428°C, and 423°C) showed strong resistance to heat before decomposing and could therefore serve as a hot packaging material [38].

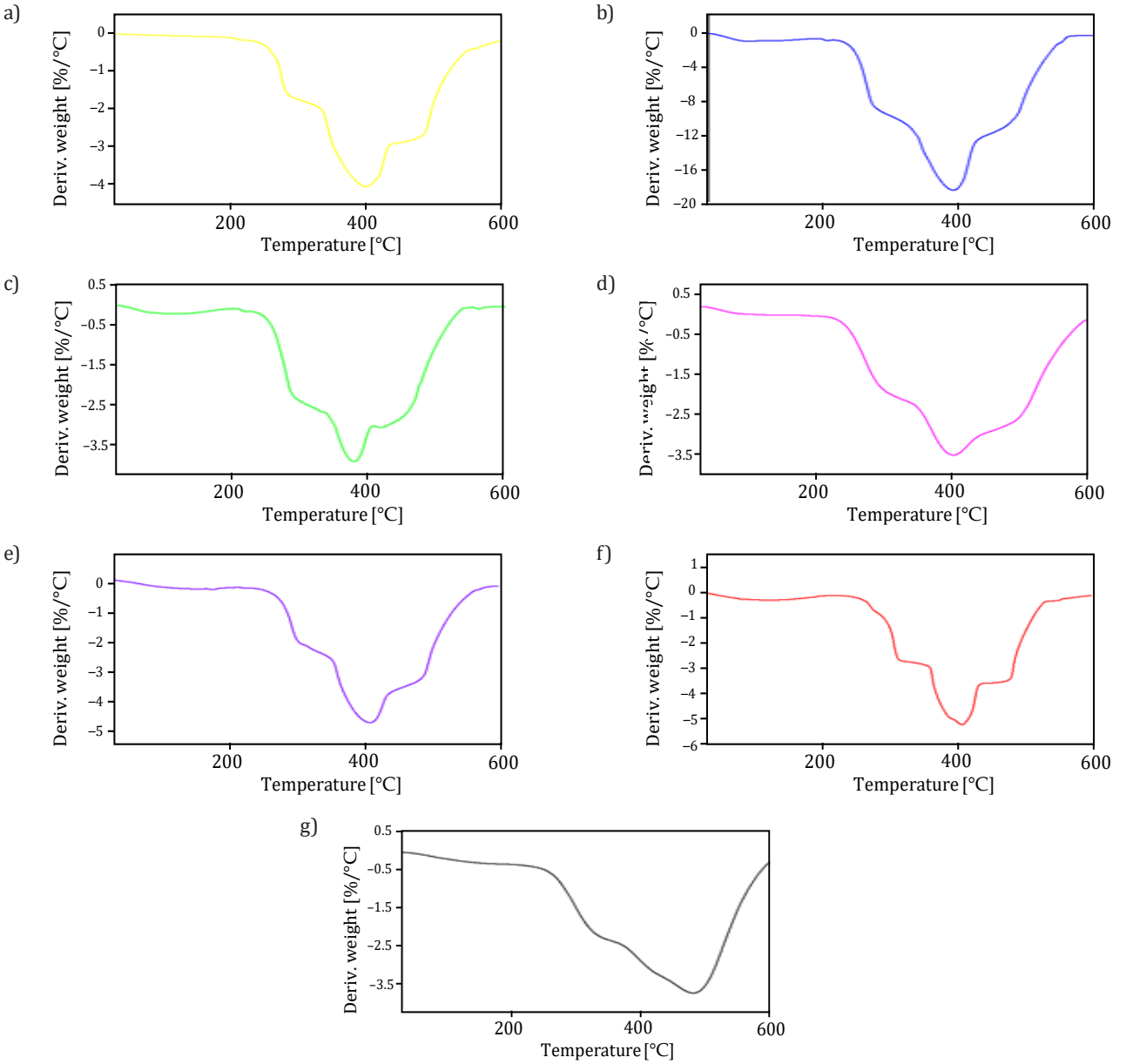

Fig. 3. DTG of electrospun PLA and the composite fibre mat: a) neat PLA; b) PLA/CHS (5 wt.%); c) PLA/CH (2.5 wt.%)/CHS (2.5 wt.%); d) PLA/CH (5 wt.%); e) PLA/CH (10 wt.%); f) PLA/CHS (10 wt.%); g) PLA/CH (5 wt.%)/CHS (5 wt.%)

3.4. Glass transition temperature (T_g) analysis of electrospun PLA and composite fibre

Figure 4 shows the DSC thermogram of electro spun PLA and PLA composites with varying percentages of reinforcement.

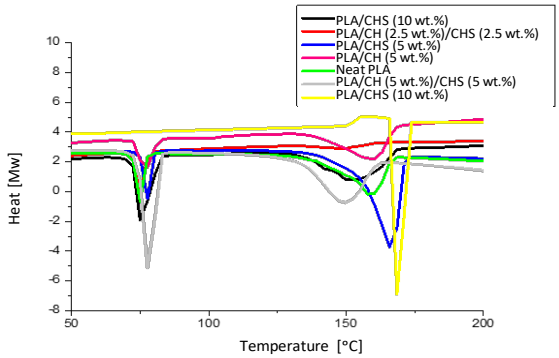

Fig. 4. DSC curve of neat PLA and composite fibre

The T_g of the neat PLA, PLA/CHS (10 wt.%), PLA/CH (2.5 wt.%)/CHS (2.5 wt.%) are the same (75°C), while that of PLA/CHS (5 wt.%),PLA/CH (5 wt.%) have a T_g of (77°C) and PLA/CH (5 wt.%)/CHS (5 wt.%) a T_g of (78°C), which are higher than that of neat PLA. PLA/CH (10 wt.%), did not show any glass transition temperature. A slight increase in the glass transition temperature of the composite shows an increase in the ductility of the reinforced fibre mat material. Thus, PLA/CHS (5 wt.%),PLA/CH (5 wt.%), PLA/CH (5 wt.%)/CHS (5 wt.%) is a suitable material for wound dressing, due to its enhanced ductility. This result is in agreement with [31] who reported a slight increase in T_g of PLA reinforced with 10 wt.% of kenaf fibre. However, T_g reported here is a little higher than the one observed in the literature [12, 23, 31]. The increase in the glass transition temperature is due to the restriction of polymer chain mobility within the interface caused by the hydrogen bonding created between the PLA fibre surface and the fibre reinforcement [39, 40]. The formation of a single glass transition temperature confirms that the composite blend is miscible. A cold crystalline peak was noticed at 155°C. For PLA/CH (10 wt.%), which was not observed in the other composites. The presence of cold crystallization has been attributed to freezing of crystallization before the completion of solvent removal from the spun fibre mat [40]. This composite possesses the lowest crystallinity (65.1%) as shown in Table 1. This was also observed in the work of [9] where the low crystallinity was attributed to the presence of cold crystallization. The melting peak for PLA/CH (5 wt.%) and neat PLA is the same (159°C); PLA/CHS (10 wt.%) and PLA/CH (2.5 wt.%)/CHS (2.5 wt.%) have their melting peak at 152°C while that of PLA/CHS (5 wt.%), PLA/CH (10 wt.%) and PLA/CHS (wt.%)/CH (5 wt.%) occurred at 165°C, 169°C and 149°C respectively. It was observed that the melting peak of PLA/CHS (10 wt.%), PLA/CH (2.5 wt.%)/CHS (2.5 wt.%) and PLA/CHS (5 wt.%)/CH (5 wt.%) is lower than that of neat PLA while PLA/CHS (5 wt.%), PLA/CH (10 wt.%) has a higher melting peak. The increase in this melting temperature might be due to the rearrangement of molecular chain in the regular crystals [12].

3.5. Morphology features of electrospun PLA and composite fibre

Figure 5 shows the electrospun fibre morphology while Figure 6 shows average fibre diameter distribution for neat PLA and its composites. The morphology reveals that the fibres were distributed randomly in a non-woven formation. The fibre diameter of the neat PLA was found to be 14.53 nm. PLA/CH (5 wt.%), PLA/CH (2.5 wt.%)/CHS (2.5 wt.%), PLA/CH (10 wt.%) have a fibre diameter of 15.95 nm, 16.85 nm, 15.15 nm respectively. The increase in fibre diameter of PLA, with the addition of reinforcement may be attributed to an increase in solution viscosity in agreement with the observation of [21].

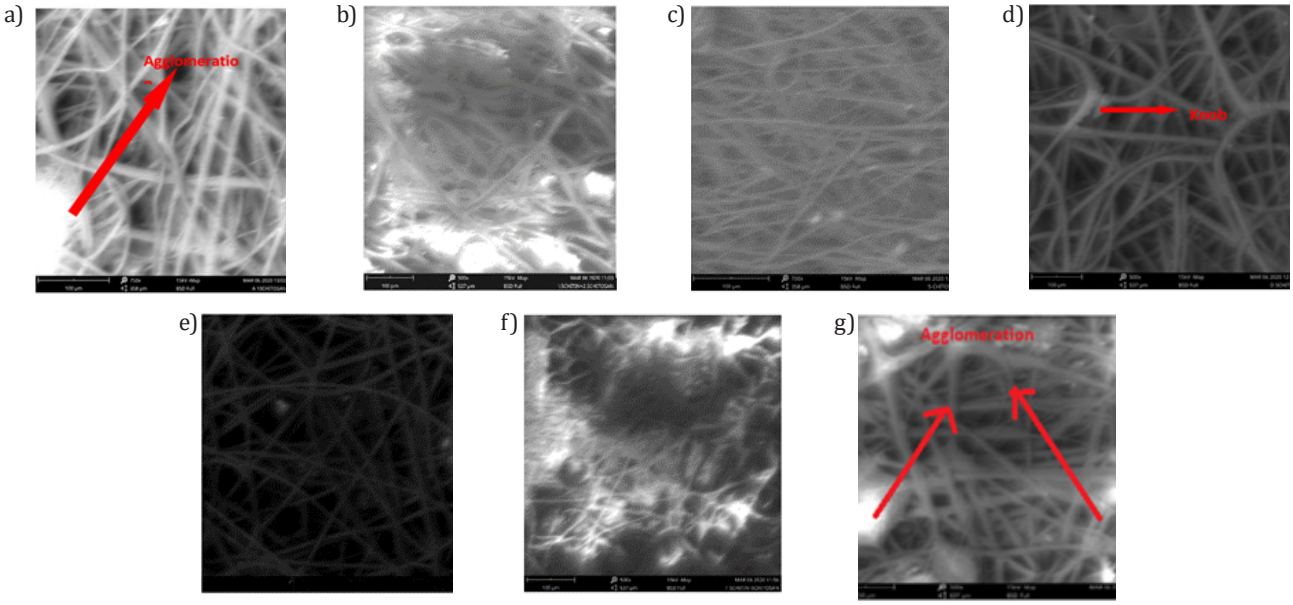

Fig. 5. The SEM morphology of: a) PLA/CHS (10 wt.%; b) PLA/CH (2.5 wt.%)/CHS (2.5 wt.%); c) PLA/CHS (5 wt.%); d) PLA/CH (5 wt.%); e) neat PLA; f) PLA/CH (5 wt.%)/CHS (5 wt.%); g) PLA/CH (10 wt.%)

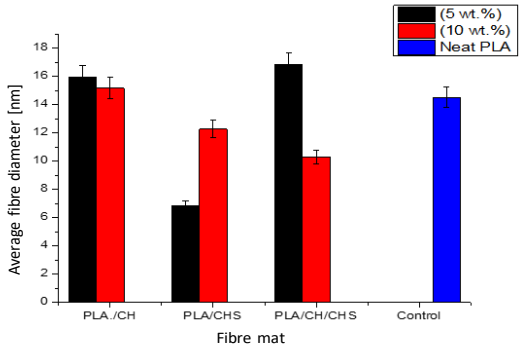

Fig. 6. Fibre diameter of electrospun fibre

Conversely, PLA/ CHS (5 wt.%), PLA/CHS (10 wt.%) and PLA/CH (5 wt.%)/CHS (5 wt.%) showed fibre diameter of 6.86 nm, 12.27 nm, and 10.29 nm respectively, which is lower than that of neat PLA. This could be attributed to the alleviation of the clogging issue arising from agglomeration during electrospinning. The fibres exhibited a relatively uniform fibre diameter. A knob was observed in PLA/CH (5 wt.%), which might be due to the agglomeration of micro-particles that did not completely dissolve in the PLA matrix [41]. The presence of beads was also noticed in PLA/CHS (5 wt.%), PLA/CH (10 wt.%) and PLA/CHS (10 wt.%). Neat PLA has an average pore diameter of 22 m, which is higher than that of the composite's fibres. The pore diameters of the composites were 16 µm, 13 µm, 11 µm, 13 µm, 10 µm and 15 µm for PLA/CHS (10 wt%), PLA/CH (2.5 wt%)/CHS (2.5 wt.%), PLA/CHS (5 wt.%), PLA/CH (5 wt.%), PLA/CH (5 wt.%)/CHS (5 wt.%) and PLA/CH (10 wt.%) respectively. The pore sizes were a result of the irregular deposition of the fibres. However, the pore diameter reported here is higher than the one reported by [24]. In the research of [36] on electrospun polylactic acid and chitosan using different solvents, they noted that a uniform fibre diameter was obtained at 0.4 wt.% chitosan. However, in this present study, a uniform fibre diameter was obtained at various weight fractions for a single solvent.

3.6. Strength characteristics of PLA and its composite

The mechanical strength of a composite nano fibre is quite important for its potential use as a wound dressing material. The tensile strengths of PLA/CH (2.5 wt.%)/CHS (2.5 wt.%) fibre and PLA/CHS (5 wt.%) are 0.60 MPa and 0.40 MPa respectively, which are superior to neat PLA (0.30 MPa), while the rest of the fibre mats have lower tensile strength. From Figure 7, it is observed that there is a minimum percentage of reinforcement for peak tensile strength (0.60 MPa) which corresponds to PLA/CH (2.5 wt.%)/CHS (2.5 wt.%) reinforcement. At 10 wt.% fraction of chitin filler, the tensile strength decreased to 0.1MPa. However, chitosan reinforcement seems to have better properties compared to chitin. A similar report was observed by [35] who electrospun a PLA scaffold coated with PVC (poly vinyl alcohol) and observed that the tensile strength of reinforced fibre mat was better than the neat PLA. The study attributed this to an increase in the tear resistance of the branched PVA fibres (i.e., web-like fibres, parallel PLA fibres bounded to each other by PVA fibres of different diameter) and fibre junctions. This report agrees with the findings of [32] where wood fibre was used to reinforce PLA. It was also noted that the tensile strength of the composite was reduced with the increase in the weight fraction of the wood fibre. Again, [17] electrospun a PLA nano-composite fibre mat with hybrid graphene oxide and nano-hydroxyapatite reinforcement and obtained a maximum tensile strength of 0.57 MPa. However, the current study showed a 5% improvement in the tensile property of PLA (0.31 MPa) fibre mat composite.

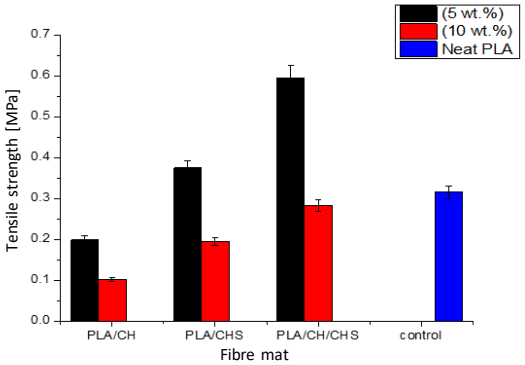

Fig. 7. Tensile strength of the electrospun fibre

3.7. Tensile energy at break

Materials used for internal body fixation should withstand long term loading, making it necessary to study the fibre tensile energy at break (TEB). The convectional testing method for toughness cannot be used as it is not a bulk material. Thus, tensile energy at break (TEB) is used as an alternative [9]. Figure 8 shows the tensile energy at break of the fibre mat. Fibre composite PLA/CH (5 wt.%)/CHS (5 wt.%), PLA/CHS (5 wt.%) and PLA/CH (2.5 wt.%)/CHS (2.5 wt.%) proved to have a superior TEB compared with the neat PLA (0.036 J).

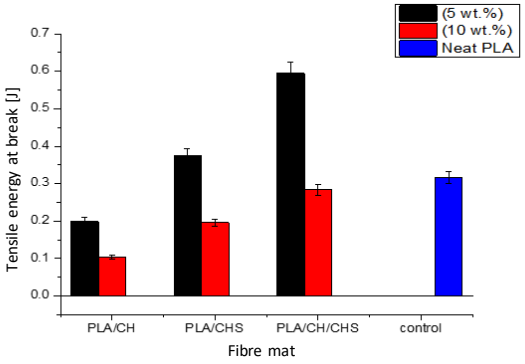

Fig. 8. Tensile energy at break

Fibre mat PLA/CH (5 wt.%)/CHS (5 wt.%) has the highest TEB (0.111 J). Tensile energy at break is a measure of material toughness. Wound dressing materials should be able to withstand long-term loading before failure, especially during the wound swelling phase. Thus, fibre mat PLA/CH (5 wt.%)/CHS (5 wt.%) with the highest TEB is recommended for large surface wounds that tend to swell more during the swelling phase without compromising the property of the material. It

was observed that the TEB is dependent on the weight percentage of the filler. Thus, 5 wt.% reinforcement shows a better TEB and good tensile strength as described above.

3.8. Strain at maximum stress

The fibre mats in Figure 9 did not show any definite pattern in relation to the weight fraction of the filler used. However, PLA/CH (5 wt.%)/CHS (5 wt.%), PLA/CHS (5 wt.%), PLA/CHS (10 wt.%) and PLA/CH (2.5 wt.%)/CHS (2.5 wt.%), showed a better strain before the material yielded. Fibre mat with PLA/CH (5 wt.%)/CHS (5 wt.%), showed the maximum strain (0.18%), which is about a 199% improvement over the neat PLA fibre mat. Thus, this material is recommended for use when the affected part undergoes continuous movement and may exert strain on the material.

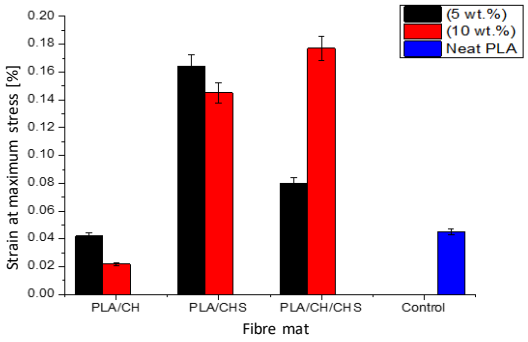

Fig. 9. Strain at maximum stress

3.9. Water absorption capacity of PLA composite

Figure 10 shows the rate of water absorption of the electrospun samples at room temperature.

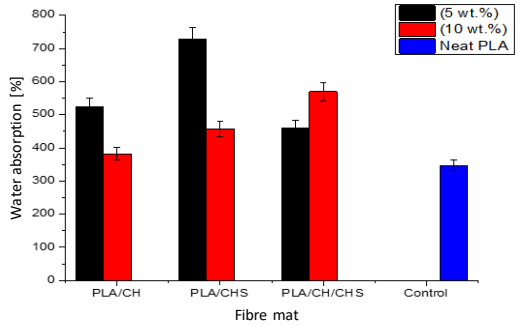

Fig. 10. Water absorption capacity of PLA and its composite

Optimum water absorption capacity was obtained at 5 wt.% chitosan in PLA. The rate of water absorption was observed to be dependent on the percentage weight of the filler. However, as filler content increases, the water absorption capacity decreases. This suggests that the composite pore spaces were more compacted as filler weight increases. Chitosan filler showed better water absorption capacity when compared to chitin in the PLA composite matrix. This improvement by chitosan may be attributed to the formation of an amino group (-NH_2) of the chitosan during deacetylation. Generally, the water absorption capacity of the composites was better than the neat PLA. It is shown by the work of [9], who earlier reported an improvement in water absorption capacity over neat PLA by reinforcing PLA with Bagasse. More importantly, the result reported here showed highest water absorption of ~750%, which is superior to that reported by [17] in a study of electrospun polylactic acid nano-composite fibre mats with hybrid graphene oxide and nano-hydroxyapatite reinforcements (~210%).

3.10. Antimicrobial test

Figure 11 shows the total viable counts (TVCs) of the bacteria exposed to composites, and unexposed bacteria. All the composites show an antibacterial effect against *staphylococcus aureus*.

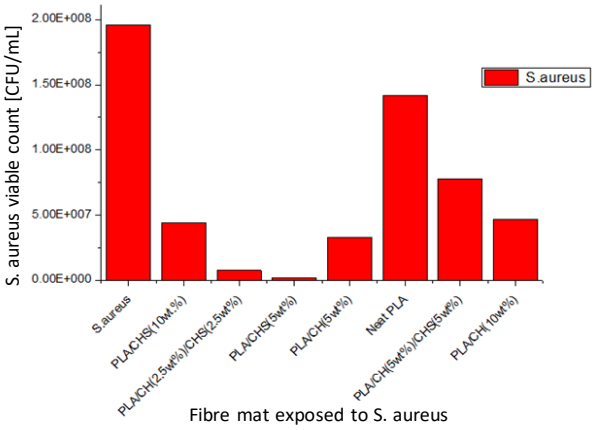

Fig. 11. The total viable counts (TVCs) bacteria exposed to composites and unexposed bacteria

The fibre mat with the composition PLA/CHS (5 wt.%) shows the highest antibacterial effect against *staphylococcus aureus*, with the highest number of reduction in the bacterial population ($1.942 \cdot 10^8$ CFU/ml). The results from this present study agrees with earlier works by [18] who fabricated a chitosan-cellulose composite for wound dressing, and reported that chitosan can effectively kill gram positive *staphylococcus aureus*. At 5 wt.% reinforcement good performance against *staphylococcus aureus* was recorded. Surprisingly, the neat PLA to an extent showed some activity against this bacterium, suggesting that unreinforced PLA has some measures of inherent antimicrobial property. The percentage reduction in the microbial population is 96.0, 99.0, 85.0, 27.0, 60.0 and 70.0% for PLA/CH (2.5 wt.%)/CHS (2.5 wt.%), PLA/CHS (5 wt.%), PLA/CH (5 wt.%), Neat PLA, PLA/CH (5 wt.%)/CHS (5 wt.%), PLA/CH (10 wt.%) respectively. Bacteriostatic and bactericidal are known to be very important in wound healing applications in preventing infection. The authors [42, 43] showed that electrospun nanofibers combining the biocompatibility potential of PVA with 0.01% w/w keratin and the antibacterial property of mupirocin was effective in treating drug resistant wounds. Hence, the PLA/CHS developed

scaffold can be used as a backbone for the development of antibacterial composites containing antibacterial agents that will enhance its antibacterial and bacteriostatic activity. This property was exhibited by chitin and chitosan reinforced PLA composites fibres, making them suitable as wound dressing materials to prevent wound colonization or severe infection. Figure 12 showed the population of staphylococcus bacteria exposed to composites, and unexposed bacteria. The bacteria were exposed to the composites for 24 hours. Physical examination showed sizable number of reductions in the population growth proving that the composites were resistant against staphylococcus aureus development and growth.

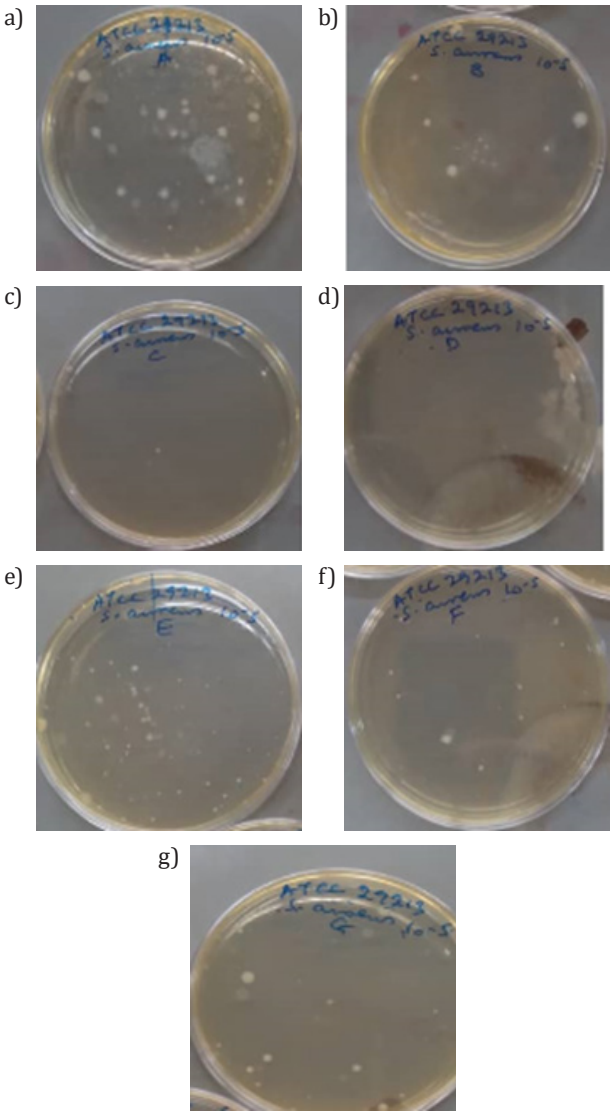

Fig. 12. Reduction in the microbial population of exposed and unexposed bacterial: a) PLA/CHS (10 wt.%); b) PLA/CH (2.5 wt.%)/CHS (2.5 wt.%); c) PLA/CHS (5 wt.%); d) PLA/CH (5 wt.%); e) neat PLA; f) PLA/CH (5 wt.%)/CHS (5 wt.%); g) PLA/CH (10 wt.%)

4. CONCLUSION

An electrospun fibre (PLA/CH/CHS) mat with good morphology suitable for surgical wound dressing was developed using 0.14 g/mL of PLA and fillers in a DCM solvent. The tensile strength of neat PLA (0.3MPa) was improved by 100%. The tensile strain of neat PLA (0.045%) was enhanced (199%) when reinforced with CHS (10 wt.%). The fibre mat has the requisite thermal stability required for wound dressing, (~185°C). The crystallinity of PLA (67.6%) declines by 3.8%, with PLA/CH (10 wt.%) with improvement in hydrophilicity of PLA as increase in water absorption capacity of the fibre mat occurred. Thus, the fibre mat produced is capable of absorbing exudate. The composite showed antibacterial resistance against *staphylococcus aureus* (99.0% efficiency) exhibited by PLA/CH (2.5 wt.%)/CHS (2.5 wt.%) fibre. This fibre mat is suitable for wound dressing to prevent wound infections and as useful backbone for the development of bioactive wound dressings.

REFERENCES

[1] Boateng J.S., Matthews K.H., Stevens H.N.E. & Eccleston G.M. (2008). Wound healing dressings and drug delivery systems: a review. *Journal of Pharmaceutical Sciences*, 97(8), 2892–2923. Doi: https://doi.org/10.1002/jps.21210.

[2] Chandan K.S. (2019). Human wounds and its Burden: An updated Compendium of Estimates. *Advances in Wound Care*, 8(2), 39–49. Doi: https://doi.org/10.1089/wound.2019.0946.

[3] Willi P. & Chandra P.S. (2004). Chitosan and Alginate Wound Dressings: A Short Review. *Trends Biomaterial Artificial Organs*, 18(1), 18–23.

[4] Ilenghoven D., Chan C.Y., Wsr W.A.K., Mohdyussof S.J. & Ibrahim S. (2017). A Review of Wound Dressing Practices. *Clinical Dermatology Open Access Journal*, 2(6), 000133. Doi: https://doi.org/10.23880/CDOAJ-16000133.

[5] Uzun M. (2018). A review of Wound Management Materials. *Journal of Textile Engineering and Fashion Technology*, 1(4), 53–59. Doi: https://doi.org/10.15406/jteft.2018.04.00121.

[6] Zahedi P., Rezaeian I., Ranaei-Siadat S.-O., Jafari S.-H. & Supaphol P. (2009). A review on wound dressings with an emphasis on electrospun nanofibrous polymeric bondages. *Polymer Advance Technology*, 21, 77–95. Doi: https://doi.org/10.1002/pat.1625.

[7] Rahman G.A., Adigun I.A., Yusuf I.F. & Ofoegbu C.K.P. (2006). Wound dressing where there is a limitation of choice. *Nigerian Journal of Surgical Research*, 8(3–4), 151–154. Doi: https://doi.org/10.4314/njsr.v8i3-4.54882.

[8] Adomavičiūtė E., Pupkevičiūtė S., Juškaitė V., Žilius M., Stanys S., Pavilonis A. & Briedis V. (2017). Formation and Investigation of Electrospun PLA Materials with Propolis Extracts and Silver Nanoparticles for Biomedical Applications. *Journal of Nanomaterials*, 1–11, 8612819. Doi: https://doi.org/10.1155/2017/8612819.

[9] Akpan E.I., Gbenebor O.P., Igogori E.A., Aworinde A.K. Adeosun S.O. & Olaleye S.A. (2019). Electrospun porous bio-fibre base on polylactide/natural fibre particles. *Arab Journal of Basic and Applied Sciences*, 26(1), 225–235. Doi: https://doi.org/10.1080/25765299.2019.1607995.

[10] Hidalago I.A., Sojo F., Arvelo F. & Sabino M.A. (2013). Functional electrospun poly(latic acid) scaffolds for biomedical applications: experimental conditions, degradation and biocompatibility study. *Molecular and cellular Biomechanics*, 10(2), 85–105. Doi: https://doi.org/10.3970/mcb.2013.010.085.

[11] Anderson J.M. & Shive M.S. (1997). Biodegradation and biocompatibility of PLA and PLG microspheres. *Advanced Drug Delivery Reviews*, 28(1), 5–24. Doi: https://doi.org/10.1016/s0169-409x(97)00048-3.

[12] Gu X., Li Y., Cao R., Liu S., Fu C., Feng, S. Yang C., Cheng W. & Wang Y. (2019). Novel electrospun Poly(latic acid)/Polybutylene/Graphene oxide nanofiber membranes for antibacterial applications advances. *AIP Advances*, 9(6), 065306. Doi: https://doi.org/10.1063/1.5100109.

[13] Eltom A., Zhong G. & Muhammad A. (2019). Scaffold Techniques and Designs in Tissue Engineering Functions and Purposes: A Review. *Advances in Materials Science and Engineering*, 3429527. Doi: https://doi.org/10.1155/2019/3429527.

[14] Thamarai S.V., Gobinath R., Thirumurugan K. & Mekala N. (2019). Development of Electrospun Wound Dressing for Hemorrhage Control using Biominerals. *International Journal of Recent Technology and Engineering*, 8(2S3), 880–882. Doi: https://doi.org/10.35940/ijrte.B1165.0782S319.

[15] Naseri N., Algan C., Jacobs V., John M. Oksman K. & Mathew A.P. (2014). Electrospun chitosan-based nanocomposites mats reinforced with chitin nanocrystals for wound dressing. *Carbohydrate Polymers*, 109, 7–15. Doi: https://doi.org/10.1016/j.carbpol.2014.03.031.

[16] Juárez-de la Rosa B.A., Quintana P., Ardisson P.I., Yáñez-Limón J.M., Alvarado-Gil J.J. (2012). Effects of thermal treatments on structure of two black coral species chitinous exoskeleton. *Journal of Material Science*, 47, 990–998. Doi: http://dx.doi.org/10.1007%2Fs10853-011-5878-9.

[17] Liu C., Wong H.M., Yeung K.W.K & Tjong S.C. (2016). Novel Electrospun Polylactic Acid Nanocomposite Fiber Mats with Hybrid Graphene Oxide and Nanohydroxyapatite Reinforcements Having Enhanced Biocompatibility. *Polymers*, 8(8), 287. Doi: https://doi.org/10.3390/polym8080287.

[18] Harkins A.L., Duri S., Kloth L.C. & Tran C.D. (2013). Chitosan-cellulose composite for wound dressing material. Part 2. Antimicrobial activity, blood absorption ability and biocompatibility. *Journal of Biomedical Material Research. Part B*, 102(6), 1199–1206. Doi: https://doi.org/10.1002/jbm.b.33103.

[19] Dubey R.C. & Maheshwari D.K. (2012). *Practical microbiology*. 2nd Edition. S. Chand and Company private ltd, (Ed.), New Delhi.

[20] Boland E.D., Pawlowski K.J., Barnes C.P., Simpson D.G., Wnek G.E. & Bowlin G.L. (2006). Electrospinning of bioresorbable polymers for tissue engineering scaffolds. *American Chemical Society Symposium Series*, 918, 188–204. Doi: http://dx.doi.org/10.1021/bk-2006-0918.ch014.

[21] Dong Y., Marshall J., Haroosh H.J., Mohammadzadehmoghadam S., Liu D., Qi X. & Lau K.-T. (2015). Polylactic acid (PLA)/halloysite nanotube (HNT) composite mats: Influence of HNTcontent and modification. *Composites Part A*: *Applied Science and Manufacturing*, 76, 28–36. Doi: https://doi.org/10.1016/j.compositesa.2015.05.011.

[22] Oliveira J.E., Mattoso L.H.C., Orts W.J. & Medeiros E.S. (2013). Structural and Morphological Characterization of Micro and Nanofibers Produced by Electrospinning and Solution Blow Spinning: A comparative study. *Advances in Materials Science and Engineering*. 409572. Doi: https://doi.org/10.1155/2013/409572.

[23] Marsi T.C.O., Ricci R., Toniato T.V., Vasconcellos L.M.R., Vaz Elias M.V., Silva A.D.R., Furtado A.S.A., Magalhães L.S.S.M., Silva-Filho E.C., Marciano F.R., Zille A., Webster T.J. & Lobo A.O. (2019). Electrospun Nanofibrous Poly (Lactic Acid)/Titanium Dioxide Nanocomposite Membranes for Cutaneous Scar Minimization. *Frontiers in Bioengineering and Biotechnology*. Doi: https://doi.org/10.3389/fbioe.2019.00421.

[24] Lu Y., Chen Y.-C. & Zhang P.-H. (2016). Preparation and characterization of Polylactic Acid (PLA)/Polycaprolactone (PCL) Composite Microfiber Membranes. *Fibres and Textiles in Eastern Europe*. 3(117), 17–25. Doi: https://doi.org/10.5604/12303666.1196607.

[25] Qi G. (2013). *Fabrication and characterization of PLA, PHBV and Chitin Nanowisker Blends, Composites and foams for High structural Applications*. University of Toronto [unpublished Master Thesis].

[26] Kancheva M., Toncheva A., Manolova N. & Rashkov I. (2015). Enhancing the mechanical properties of electrospun polyester mats by heat treatment. *Express Polymer Letters*, 9(1), 49–65. Doi: https://doi.org/10.3144/expresspolymlett.2015.6.

[27] Ahyat N.M., Mohamad F., Ahmad A.S. & Azmi A.A. (2017). Chitin and Chitosan Extraction from Portunus Pelagicus. *Malaysian Journal of Analytical Sciences*, 21(4), 770–777. Doi: https://doi.org/10.17576/mjas-2017-2104-02.

[28] Gbenebor O.P., Adeosun S.O., Lawal G.I., Jun S. & Olaleye S.A. (2017). Acetylation, crystalline and morphological properties of structural polysaccharide from shrimp exoskeleton. *Engineering Science and Technology, an International Journal*, 20(3), 1155–1165. Doi: https://doi.org/10.1016/j.jestch.2017.05.002.

[29] Gonçalves R.P., Ferreira W.H., Gouvêa R.F., & Andrade C.T. (2017). Effect of chitosan on the properties of electropunk fibers from mixed poly(Vinyl Alcohol)/chitosan solution. *Materials Research*, 20(40), 984–993. Doi: https://doi.org/10.1590/1980-5373-MR-2016-0618.

[30] Pawlak A. & Mucha M. (2003). Termogravimetric and FTIR studies of chitosan blends. *Termochimica Acta*. 396(1–2), 153–166. Doi: https://doi.org/10.1016/s0040-6031(02)00523-3.

[31] Tawakkal M.A. (2016). Characterization and antimicrobial activity of poly (lactic acid)/kenaf bio-composites containing a natural agent. Vectorial University Melbourne, Australia [unpublished Doctoral Thesis].

[32] Huda M.S., Drzal L.T., Misra M. & Mohanty A.K. (2006). Wood-fiber-reinforced poly (lactic acid) composites: Evaluation of the physiochemical and morphological properties. *Journal of Applied Polymer Science*, 102(5), 4856–4869. Doi: https://doi.org/10.1002/app.24829.

[33] Abdelaal O.A., & Darwish S. M. (2013). Review of Rapid Prototyping Techniques for Tissue Engineering Scaffolds Fabrication. In: *Öchsner* A., da Silva L.F.M. & Altenbach H., *Characterization and Development of Biosystems and Biomaterials*, Springer-Verlag, Berlin – Heidelberg, 33–54.

[34] Meneghello G., Parker D.J., Ainsworth B.J., Perera S.P., Chaudhuri J.B., Ellis M.J. & De Bank P.A. (2009). Fabrication and characterization of poly(lactic-*co*-glycolic acid)/polyvinyl alcohol blended hollow fibre membrane for tissue engineering applications. *Journal of Membrane Science*, 344(1–2), 55–61. Doi: http://dx.doi.org/10.1016/j.memsci.2009.07.034.

[35] Abdal-hay A., Hussein K.H., Casettari L., Khalil K.A & Hamdy A.S. (2015). Fabrication of novel high performance ductile poly(lactic acid) nanofiber scaffold coated with poly(vinyl alcohol) for tissue engineering application. *Material Science and Engineering: C*, 60, 143–150. Doi: https://doi.org/10.1016/j.msec.2015.11.024.

[36] Thomas M.S., Pillai P.S.K., Faria M., Cordeiro N., Barud H., Thomas S. & Pothen L.A. (2018). Electrospun polylactic acid-chitosan composite. A bio-based alternative for inorganic composites for advance application. *Journal of Material Science: Materials in Medicine*, 29:137. Doi: https://doi.org/10.1007/s10856-018-6146-1.

[37] Silverajah V.S, Ibrahim N.A., Yunus W.Z.W., Hassan H.A. & Woei C.B. (2012). A comparative study on the mechanical, thermal and morphological characterization of poly(lactic acid)/epoxidized palm oil blend. *International Journal of Molecular Sciences*, 13(5), 5878–5898. Doi: https://doi.org/10.3390/ijms13055878.

[38] Murariu M., Dechief A.-L., Ramy-Ratiarison R., Paint Y., Raquez J.-M. & Dubois P. (2015) Recent advances in production of poly (lactic acid) (PLA) nanocomposites: a versatile method to tune crystallization properties of PLA. *Nanocomposites*, 1(2), 71–82. Doi: https://doi.org/10.1179/2055033214Y.0000000008.

[39] Hossain K.M.Z., Felfel R.M., Rudd C.D., Thielemans W. & Ahmed I. (2014). The effect of cellulose nanowhiskers on the flexural properties of self-reinforced polylactic acid composites. *Reactive & Functional Polymer*, 85, 193–200.

[40] Chen H.-C., Tsai C.-H. & Yang M.-C. (2011). Mechanical properties and biocompatibility of electrospun polylactide/poly(vinylidene fluoride) material. *Journal of Polymer Research*, 18(3), 319–327. Doi: https://doi.org/10.1007/s10965-010-9421-5.

[41] Zhao N., Shi S., Lu G. & Wei M. (2007). Polylactide (PLA)/layered double hydroxides composite fibers by electrospinning method. *Journal of Physics and Chemistry of Solids*, 69(5–6), 1564–1568. Doi: https://doi.org/10.1016/j.jpcs.2007.10.046.

[42] Amajuoyi J.N., Ilomuanya M.O., Asantewaa-Osei Y., Azubuike C.P., Adeosun S.O. & Igwilo C.I. (2020). Development of electrospun Keratin/coenzyme Q10/poly vinyl alcohol nano fibrous scaffold containing mupirocin dressing for infected wounds. *Future Journal of Pharmaceutical Sciences*, 6(25). Doi: https://doi.org/10.1186/s43094-020-00043-z.

[43] Ilomuanya M.O., Okafor P.S., Amajuoyi J.N., Onyejekwe J.C., Okubanjo O.O., Adeosun S.O. & Silva B.O. (2020). Polylactic acid--based electrospun fiber and Hyaluronic acid-valsartan hydrogel scaffold for chronic wound healing. *Beni-Suef University Journal of Basic and Applied Sciences*, 9(31). Doi: https://doi.org/10.1186/s43088-020-00057-9.